1470 *KSME International Journal, Vol. 16 No. 11, pp. 1470~1476, 2002*

Flow-Dependent Friction Loss in an Implantable Artificial Lung

Sam Cheol Lee*

Department of Advanced Materials Engineering, Hanlyo University, Kwangyang, Kwangyang-Si, Chonnam 545-704, Korea

The goal of this work is to design and build an implantable artificial lung that can be inserted as a whole into a large vein in the body with the least effect on cardiovascular hemodynamics. The experimental results demonstrate that the pressure drop is not entirely related to viscosity effects. The friction factor decreases with an increase in the number of tied-hollow fibers at a constant Reynolds number. A uniform flow pattern without stagnation is observed at all numbers of tied hollow fibers tested. The tied hollow fiber module, built in this study with 3 cm of outer diameter of module, 380 m of outer diameter of tied hollow fiber, and 700 number of tied hollow fiber with length of 60 cm, which shows a pressure drop of 13-16 mmHg, satisfies the required pressure drop qualifying 15 mmHg as an intravascular artificial lung.

Key Words: Implantable Artificial Lung, Severe Respiratory Failure, Pulmonary Circulation, Optimum Design, Pressure Drop, Friction Loss, Tied-Hollow Fiber

Nomenclature

A : Membrane surface area
A_f : Frontal area of the blood path
d : Diameter of the fiber
D_I : Inside housing outer diameter
D_O : Outer housing inner diameter
f : Friction factor
L : Length of the fiber compartment
N_{Re} : Reynolds number
p : Device porosity
Q : Flow rate
Q_b : Blood flow rate
R_h : Hydraulic diameter
$\triangle P$: Measured pressure drop
v : Kinetic viscosity

1. Introduction

Currently, the only way to manage patients with severe acute respiratory failure is extracorporeal life supports (ECLS) or extracorporeal membrane oxygenation (ECMO) (Bartlett 1990). So far, the only treatment for end-stage chronic lung disease such as chronic obstructive pulmonary disease (COPD), emphysema, cystic fibrosis, and idiopathic pulmonary fibrosis is lung transplantation (Borst and Schfers 1993). Lung transplantation has progressed from an investigational modality to a well established clinical application that has a potential to save patients with end-stage respiratory failure. Unfortunately, many patients who would benefit from transplantation are those with prolonged mechanical ventilatory support and therefore therapy is limited by the risk of infection. In addition, donor availability is a major limiting factor in lung transplantation, since only one out of four organ donors is a suitable lung donor (Egan et al. 1992).

ECLS has been used occasionally as a bridge to transplant and is certainly feasible; however, this technique has been used to manage patients who often require long-term intensive care unit (ICU) stays and pose a high risk for infection, creating the aforementioned contraindications to lung plantation. ECLS is also labor intensive,

* Corresponding Author,
E-mail : sclee777@hanmail.net
TEL : +82-61-760-1164; **FAX** : +82-61-761-6709
Department of Advanced Materials Engineering, Hanl yo University, Kwangyang, Kwangyang-Si, Chonnam 545-704, Korea. (Manuscript **Received** October 27, 2001; **Revised** July 24, 2002)

expensive, subject to mechanical breakdown, and may prompt the release of many inflammatory mediators (Kirklin et al. 1983) that would limit the available candidates for transplant. Clearly, the bridging modality and the transplant should be complementary, as in the case of hemodialysis and renal transplantation, whereas ECLS and lung transplantation are opposite by relative contraindications.

An implantable, artificial lung unit with the technology of ECMO is required for lung transplantation (Federspiel et al. 1999 ; Mortensen and Berry 1989). The most important potential of this system is its immediate application as a research tool. It can also be used for acute respiratory failure. With a gas exchange device powered by the right ventricle, it may be possible to separate pulmonary gas exchange functions from the other metabolic functions of the lung without introducing variables such as those associated with an extracorporeal circuit and mechanical pump. By utilizing different models of lung injury, a wide variety of experiments is also possible.

This work focuses on the assessment of the requirements based on the hydrodynamic characteristics, including hemodynamics effects of the implanted device on cardiopulmonary circulation.

Also, this work describes the hydrodynamic characteristics of an implantable artificial lung with the least effect on cardiovascular hemodynamics when it is used in line with pulmonary circulation.

2. Dimension Analysis

An artificial lung can be characterized by different geometric parameters: membrane surface area, A ; diameter of the fiber, d ; length of the fiber compartment, L ; inside housing outer diameter, D_i ; outside housing inner diameter, D_o; and frontal area of the blood path, A_f. The "void fraction" or device porosity, p, is defined as the ratio of the volume of voids (volume in the membrane compartment occupied by blood) to the volume of the bed (total volume of the membrane compartment). A characteristic length for flow through porous beds or packed fiber bundles is hydraulic radius, R_h. The hydraulic radius is expressed in terms of a volume of voids per volume of bed, p, and the wetted surface per unit volume of bed, a, (Bird et al. 1960 ; Ergun 1954)

$$R_h=\frac{p}{a}=\frac{\left(\frac{volume\ of\ voids}{volume\ of\ bed}\right)}{\left(\frac{wetted\ surface}{volume\ of\ bed}\right)}$$

The measured pressure drop, ΔP, and flow rate, Q, relationship is presented as a polynomial of second order :

$$\Delta P=a'\cdot Q^2+b'\cdot Q \tag{1}$$

Reynolds number, N_{Re}, is defined as the ratio of inertial and viscous forces. Characteristic length in the Reynolds number for flow through a fiber stack is hydraulic diameter, R_h. Consequently, Reynolds number, N_{RE}, is defined as

$$N_{Re}=\frac{Q_b d_o}{(1-p)A_f v} \tag{2}$$

in which Q_b (L/min) is the blood flow rate, d_o the outer diameter of individual fibers, p the device porosity (i.e., the void fraction), A_f (cm^2) the gross frontal area of the blood path, and v(cm^2/sec) is the kinetic viscosity of the blood. The other terms have previously been defined.

The design of a hollow fiber lung must also consider the blood-side pressure loss. For porous media. a friction factor, f, may be defined by

$$f=\frac{pd\Delta P}{2(1-p)\rho v^2 L} \tag{3}$$

in which ΔP is the blood side pressure drop, v the average velocity in the free-flow area, ρ the blood density, and L is the blood path length. The characteristic length used in this expression for f, as well as in the relations for the Reynolds number and the Sherwood number, is the hydraulic diameter, d_H, which can be shown to equal $d_H=pd/(1-p)$ for porous beds or packed fiber bundles.

For low Reynolds numbers, the friction factor has been found to be related to the Reynolds number by

$$f = \alpha N_{Re}^{\beta} \quad (4)$$

in which N_{Re} is the Reynolds number, and α and β are empirically determined constants specific for a particular geometric configuration of hollow fiber lung (e.g. α and β vary with different fiber packing densities)

3. Technical Data on an Implantable Artificial Lung

Figure 1 shows the schematic diagram of an artificial lung device designed in this experiment. The artificial lung devices consist of tied hollow fibers in a bundle varying from one (50 fibers) to four (700 fibers). The tied hollow fibers were located at equal distances inside a bundle. The artificial lung device was made of microporous polypropylene with an inner diameter of 380 μm and a membrane thickness of 50 μm (Oxyphane, Enka, Germany). Axial length and inner diameter of the artificial lung device were 600 mm and 30 mm, respectively. A core with a 30 mm diameter was placed at the center axis of the artificial lung device for uniform flow of blood. The void fraction of the hollow fiber membrane, p, which was the ratio of the space to the total volume of the artificial lung, was approximately 45%.

4. Measurement of Blood Pressure Drop Using Blood Substitutes

Figure 2 shows the schematic diagram of the experimental circuit for the measurement of blood pressure drop. The circuit was flushed first with carbon dioxide. Approximately 3700 mL of deionized water was added to a polypropylene reservoir (Model HVRF-3700, COBE Cardiovascular, USA) and was allowed to drain by gravity. Water was then pumped by a roller pump (Model 7520-00, Cole-Parmer Instrument, USA) and a speed controller (Model 7553-71, Cole-Parmer Instrument, USA) through 1/4″×1/16″ polyvinyl chloride laboratory tubing (Norton Co., USA). During the recirculation phase, water was returned to the inlet reservoir while it was deoxygenated and warmed to 37 ℃ by an integral heat exchanger (Model CE 0086, COBE Cardiovascular, USA) and a circulation water bath (Model 12105-30, Cole-Parmer Instrument, USA) on the deoxygenator. Deoxygenation was accomplished by using nitrogen as a ventilating gas.

Once the desired inlet conditions were reached, the test phase began. A single pass technique was used, in which the water exiting from the test module was recycled. The ventilating gas was

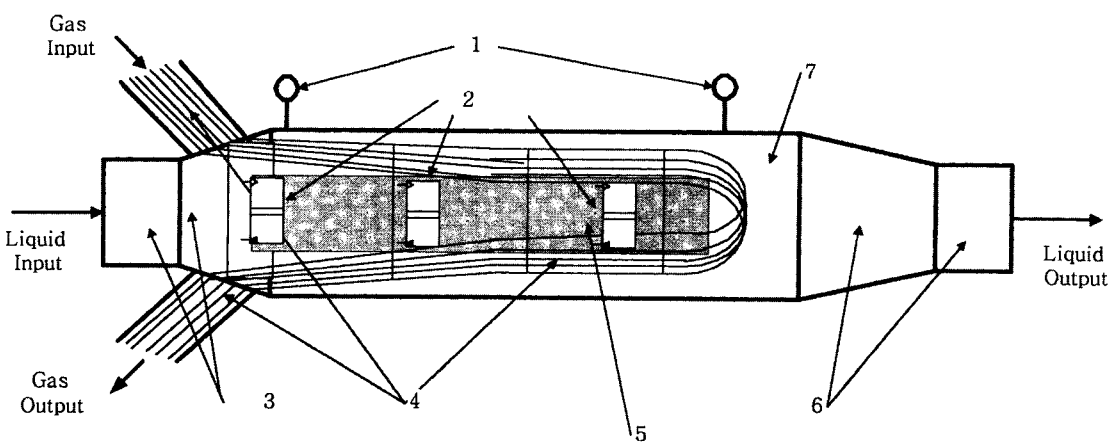

1. Pressure sensor 2. Actuator 3. Input cap 4. Hollow fiber membrane 5. Polymer plate 6. Output cap 7. Main body

Fig. 1 The schematic diagram of the artificial lung device designed in this experiment

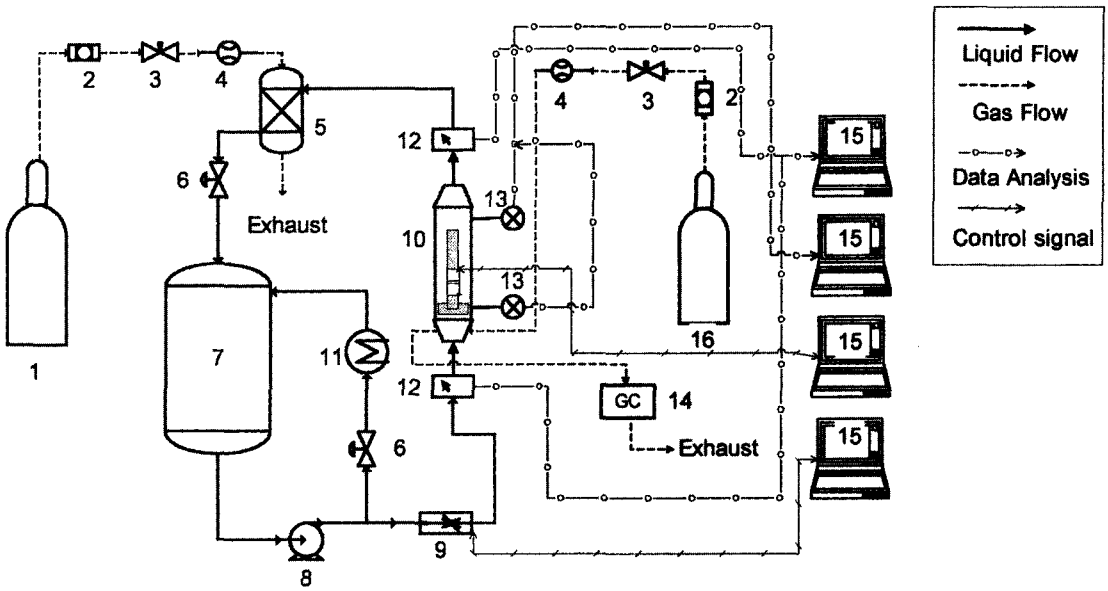

1. Gas bomb 2. Gas filter 3. Valve 4. Flow meter 5. Deoxygenator 6. Valve 7. polypropylene reservoir 8. Pump 9. Flow controller 10. Test module 11. Heat exchanger 12. Sampling port 13. Pressure sensor 14. Gas Chromatograph 15. Computer

Fig. 2 The schematic diagram of the experimental circuit for the measurement of blood pressure drop

switched to a mixture of 40-50% O_2 in N_2 as measured by an in-line O_2 analyzer (Instrumentation Laboratory, Lexington, MA, USA). After purging the sample lines, duplicate inlet and outlet water samples were taken at each of three different flow rates.

The test loop consists of a 2.54 cm diameter compliant tube in which devices were placed and perfused with distilled water at flow rates from 0.75~6 L/min at 37 ℃. Two pressure sensors ware positioned along the test module as indicated in the diagram.

Pressure drop was measured following the same protocol with exception of using 40% glycerol solution in the test circuit, which had a viscosity of 3 cps and thus better approximated the pressure drop in blood.

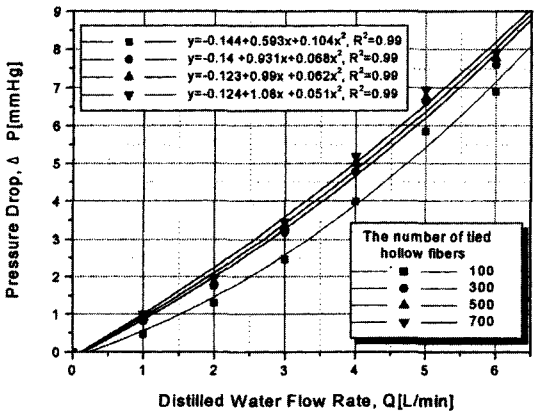

Fig. 3 Pressure drop and flow rate characteristics at the varying numbers of tied hollow fibers in distilled water at 37 ℃

5. Results

Figures 3 and 4 present pressure drop and flow rate characteristics at the varying numbers of tied hollow fibers in distilled water (Fig. 3) and in 40% glycerol solutions (Fig. 4), indicating a parabolic relationship between ΔP and Q Eq. (1). The technique to measure the pressure between the heat exchanger and the membrane compartment did not affect the pressure drop-flow rate relationship. Hence, the variance in the pressure drop-flow rate relationship in four artificial lungs with different numbers of tied hollow fibers, ranging from 100 to 700, may be attributed

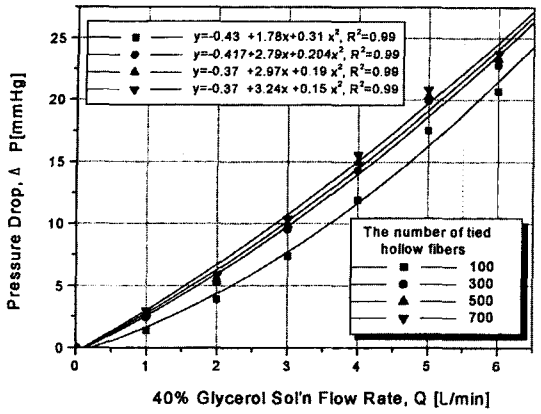

Fig. 4 Pressure drop and flow rate characteristics at the varying numbers of tied hollow fibers in 40% glycerol solution at 37 ℃

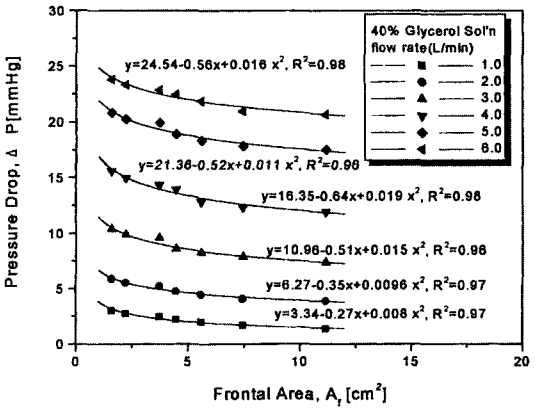

Fig. 6 The relation of pressure drop through fiber bundles to frontal area at various blood flow rates in 40% glycerol solution at 37 ℃

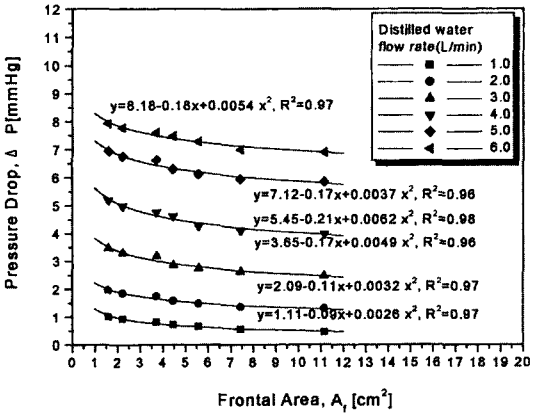

Fig. 5 The relation of pressure drop through fiber bundles to frontal area at various blood flow rates in distilled water at 37 ℃

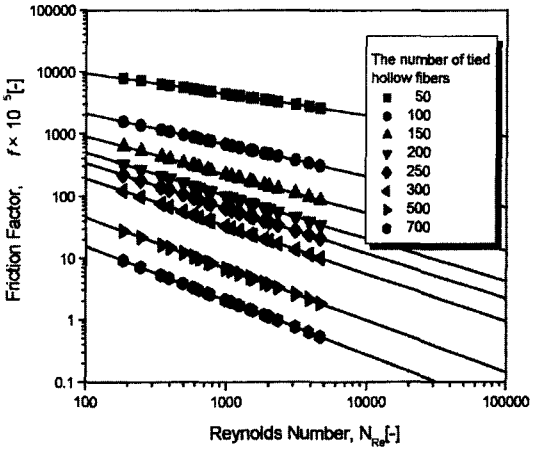

Fig. 7 The relationship between friction factor calculated by Equation (3) and Reynolds number at the varying numbers of tied hollow fibers at 37 ℃

to the difference in construction of the membrane compartment. The highest mean pressure drop in water at 4 L/min was less than 5 mmHg. In the 40% glycerol solution, the highest mean pressure drop at 4 L/min was less than 15 mmHg. Under a comparable flow rate, the highest mean pressure drop in the glycerol solution was about 3 times that of water.

Figures 5 and 6 show the relationship of a pressure drop through fiber bundles to the frontal area at various blood flow rates in distilled water (Fig. 5) and in glycerol solution (Fig. 6). The pressure drop inside the lung is clearly influenced by the liquid path length and, to a lesser extent, by the frontal area, such that a decrease in path length or an increase in frontal area results in a lower pressure drop for a given liquid flow rate. It must be noted that these data are valid only for a device made with fibers with a 30 mm outer diameter and with a fiber bundle porosity of 0.45. Figure 7 shows the relationship between the friction factor calculated by Eq. (3) and Reynolds number at varying numbers of tied hollow fibers. The friction factor was decreased with an increase in the number of tied hollow fibers at a constant Reynolds number. Uniform flow pattern

without stagnation was observed at all numbers of tied hollow fibers tested.

6. Discussion

Although some adult respiratory distress syndrome (ARDS) patients can be successfully treated by conventional mechanical ventilation, high airway pressures and highly inspired O_2 concentrations can be detrimental to lung healing. Other therapeutic options of mechanical ventilation, such as ECMO and extracorporeal CO_2 removal (ECCOR), have not gained widespread acceptance either. As an alternative approach, it is possible to eliminate the extracorporeal circuit by bringing the exchange surface to the blood within the vasculature. However, the relationship between gas transport and blood-side pressure drop must be considered due to the limited intravascular space in the aorta or vena.

This work has focused on the design requirements based on hydrodynamic characteristics, including the hemodynamic effects of the implanted device on cardiopulmonary circulation. The experimental results demonstrate that the pressure drop is partially related to density loss but not entirely to viscosity effects.

The use of this experimental data enables one to determine the optimal path length, frontal area, and surface area at a specified pressure drop. It should be noted that the pressure drop in these figures was obtained through the fiber bundle and did not include the minor losses through the inlet and outlet connectors. These minor losses would have to be added to the pressure drop through the bundle, but were considered insignificant and depended on the specific design of the connectors. For an implantable, intrathoracic lung to be feasible without addition of a prosthetic blood pump, the pressure drop must be low, on the order of 15 mmHg (Vaslef et al., 1994). In this work, the tied hollow fiber module, built in this study with 3 cm of outer diameter of module, 380 μm of outer diameter of tied hollow fiber, and 700 number of tied hollow fiber with length of 60 cm, which showed a pressure drop of 13-16 mmHg at 4 L/min, satisfies the required pressure drop qualifying 15 mmHg as an intravascular artificial lung.

Eq. (4) can then be written as;

$$f=f(N_{Re})$$

That is, the friction factor is a unique function of the Reynolds number for smooth pipe flow of all incompressible Newtonian Fluids. This result is of the greatest engineering importance, and only two groups of variables need to be studied experimentally to obtain a relation that is universally valid for a wide class of fluids and geometric and flow parameters. Dimensional analysis can indicate what dimensionless variables are related, but it cannot provide any information on the form of the relation. This must be determined either from experiment or a more fundamental analysis of the process.

As shown in Fig. 7, the friction factor relates to the Reynolds number inversely. This data have confirmed the similar data obtained previously from a broad area, such as viscosities, densities, and pipe diameters.

7. Conclusion

In this work, an implantable artificial lung was designed and built for possible use as a bridge to lung transplantation in chronic pulmonary insufficiency or as a bridge to the natural healing process in advanced adult respiratory failure. The tied hollow fiber module showed a pressure drop of 13-16 mmHg at 4 L/min, satisfie the required pressure drop qualifying 15 mmHg as an intravascular artificial lung. Other considerations that will have to be addressed in future studies include the design requirements based on oxygen transport, carbon dioxide transport, the optimal level and means of anticoagulation, and the evaluation of fiber surface coating to prevent plasma leakage and device failure.

Acknowledgment

This work was supported by grant No. R05-2000-000-00385-0 from the Korea Science & Engineering Foundation.

References

Bartlett, R. H., 1990, "Extracorporeal Life Support for Cardiopulmonary Failure," *Curr. Probl. Surg*. Vol. 27, pp. 623~705.

Bird, R. B., Stewart, W. E. and Light, E. N., 1960, *Transport phenomena*. New York, Wiley & Song, Inc., New York, pp. 180~201.

Borst, H. G. and Schfers, H. J., 1993, "Lung Transplantation," *Cli. Invest*. Vol. 71, pp. 98~101.

Egan, T. M., Boychuk, J. E., Rosato, K. and Cooper, J. D., 1992, "Whence the Lungs? A Study to Assess Suitability of Donor Lungs for Transplantation," *Transplantation*, Vol. 53, pp. 420~422.

Ergun, S., 1954, "Fluid Flow through Packed Columns," *Chem. Eng. Prog*., Vol. 48, pp. 89~94.

Federspiel, William J., Lund, L. W., Bultman, J. A., Wanant, S., Matoney, J., Golob, J. F., Frankowski, B. J., Watach, M., Litwak, P. and Hattler, B. G., 1999, "Ex-vivo Testing of the Intravenous Membrane Oxygenator(IMO)," *ASAIO J*., Vol. 45, No. 2, p. 127.

Kirklin, J. K., Westely, S., Blackstone, E. M., Kirklin, J. W., Chenoweth, D. E. and Pacifico, A. D., 1983, "Complement and the Damaging Effects of Cardiopulmonary Bypass," *J. Thorac. Cardiovasc. Surg*. Vol. 86, pp. 845~857.

Mortensen, J. D. and Berry, G., 1989, "Conceptual and Design Features of a Practical, Clinically Effective Intravenous Mechanical Blood Oxygen/carbon Dioxide Exchange Device(IVOX)," *The Intern. Artif. Organs*, Vol. 12, No. 6, pp. 384~389.

Vaslef, S. N., Mockros, L. F., Cook, K. E., Leonard, R. J., Sung, J. C. and Anderson, R. W., 1994, "Computer-Assisted Design of an Implantable, Intrathoracic Artificial Lung," *Artif. Organs*, Vol. 18, No. 11, pp. 813~817.